Observing stellar streams made in a supercomputer

Erik Fridén

Lund Observatory
Lund University

2021-EXA182

Degree project of 15 higher education credits
May 2021

Supervisor: Florent Renaud

Lund Observatory
Box 43
SE-221 00 Lund
Sweden

Abstract

Stellar streams are made of stars that originate from globular clusters or dwarf satellite galaxies that have been disturbed by the gravitational pull from the galaxy they orbit. These stellar streams hold information about the history of the progenitor as well as information about the gravitational potential of the host galaxy. In this thesis we make use of the high resolution cosmological zoom simulation VINTERGATAN, to detect and study stellar streams. Different approaches are used for the detections of stellar streams. The first method that we use is similar to what is done observationally. This includes looking at metallicity, velocity, energy, and angular momentum. In the second method used we trace back in time the particles belonging to the progenitor before its infall towards the final host galaxy. This method has a much higher accuracy and allows for deeper analysis of the stream's properties. It also allows us to evaluate the performance of the first detection method and identify eventual misinterpretation that may arise using these methods.

In this work we find that many of the larger satellites do have associated streams, but for the smaller clusters and satellites there are still many that lack any visible tidal tails. Here we detect and analyse four streams in depth: all show different characteristics such as star formation histories, metallicity, and masses. We find a diversity in age and metallicity in the stellar populations of the stream and progenitor, but one structure alone (stream or progenitor) is not always representative of the full population. The results from this work illustrate the diversity of stellar populations in streams as well as their progenitors, and the complexity of inferring the formation history of our Milky Way and its satellites from the observations of these structures.

Populärvetenskaplig beskrivning

Massan i vår galax Vintergatan, består av en idag stor del okänd massa som kallas mörk materia. Den mörka materian motsvarar ungefär 80% av den totala massan i vår galax. Att ta reda på naturen till denna mörka materia är idag ett hett forskningsområde i både astrofysik och partikelfysik. Trots årtionden av experiment med mål att hitta dessa partiklar som denna massa består av har vi än idag gått utan resultat. Dagens bevis för mörk materia har sitt ursprung inom astronomiska observationer där vi ser dess effekt från gravitationen som påverkar all massa i galaxen. Om vi skulle veta hur denna mörka materia är distribuerad inom vår galax, så skulle detta ge värdefull information om den mörka materians natur. För att studera hur den mörka materian är distribuerad inom galaxen måste vi ha något objekt för att undersöka galaxens halo och utkanter där denna massa dominerar. I galaxens halo finns det få stjärnor och strukturer vilket gör sökandet efter denna massa svår, men på senare år har antalet observerade stjärnströmmar i Vintergatan ökat kraftigt med nya observationer som tränger djupare i galaxen. Dessa stjärnströmmar kan innehålla information om hur denna mörka materia är distribuerad.

Stjärnorna i dessa stjärnströmmar har sitt ursprung från stjärnhopar eller mindre dvärggalaxer. Dessa stjärnhopar befinner sig utspritt i den galaktiska halon och är bundna till Vintergatan via dess gravitation. När gravitationen från Vintergatan drar i dessa stjärnhopar kan stjärnor lämna stjärnhopen och bli fri från dess gravitation. Detta kan liknas med hur månens gravitationskraft drar i jorden och vi ser dess effekter på havet, det vi kallar tidvatten. Med tiden kan fler och fler stjärnor lämna stjärnhopen och bilda något vi kallar för en stjärnström som har sitt ursprung från en enda stjärnhop. Genom att studera dessa stjärnströmmar kan gravitationsfältet i Vintergatan kartläggas utmed dessa stjärnströmmar. Avvikelser i stjärnströmmen kan indikera störningar i den globala gravitationspotentialen. Dessa störningar kan då bero på substrukturer av mörk materia i galaxen. Ett av problemen med stjärnströmmar idag är att de är svåra att detektera då de befinner sig långt bort från den galaktiska ljusstarka disken.

I detta arbete använder vi oss av en kosmologisk simulering för att detektera och undersöka dessa stjärnströmmar. Simuleringen är av skapandet av en galax som liknar Vintergatan i storlek, massa, samt flera andra liknande egenskaper. Från data skapad i denna simulering kommer stjärnströmmar först att detekteras med hjälp av olika metoder. I detta arbete kommer vi jämföra de stjärnströmmar som detekterats via dessa metoder. Stjärnströmmarnas egenskaper kommer analyseras ihop med dess ursprungliga stjärnhop eller dvärggalax. Målet med arbetet är att se hur vi kan detektera dessa stjärnströmmar samt finna problem som kan skapas vid detektioner av dessa stjärnströmmar. Problemen kan till exempel härstamma från egenskaperna hos dess stjärnpopulation samt skillnader mellan stjärnpopulationer inom samma struktur.

Contents

1 Introduction

Understanding the structure and evolution of our Galaxy, the Milky Way, is a central research topic in astrophysics and has been for many years. A better understanding of the Milky Way also gives a deeper understanding on the evolution and structure of galaxies in general, where there are still many unanswered questions. Research today shows that the mass distribution in galaxies is dominated by an unknown form of matter called dark matter. This dark matter is more abundant of a factor five compared to the normal baryonic matter at large scales in the Universe (Schumann, 2019).

However, there is no identification of what this dark matter is, nor its nature. Despite decades of searches for a dark matter particle, the only evidence for its existence today is indirect. There is plenty of indirect evidence from astronomy with observations done on galactic and larger scales. Since dark matter does not interact electromagnetically (or very weakly interacts) with baryonic matter, the evidence comes from its gravitational effects on its surroundings. Therefore, knowing the distribution of dark matter in galaxies would provide useful constraints on its nature, and on the formation of galaxies. The distribution could also show if it is consistent with today's theories such as the ones predicted by the standard Lambda cold dark matter cosmology (Springel et al., 2008). To study the dark matter distribution in the Galaxy there is a need for some tool to probe the Galactic halo. With the lack of structures in the Galactic halo, stellar streams have some unique properties that allow us to probe the gravitational field in the halo and the outskirts of galaxies.

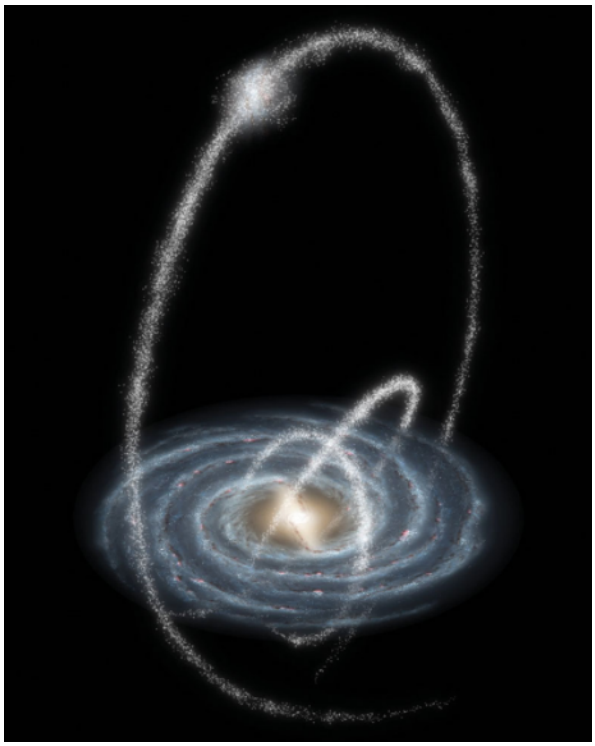

Figure 1: An artists illustration of stellar streams around a spiral galaxy. Image credit: NASA / JPL-Caltech / R. Hurt, SSC & Caltech.

Stellar streams consist of stars that have been stripped away from their original host. This can be a globular cluster or a satellite galaxy. Streams can be seen as a small overdensity of stars creating a path or trace in the sky. An artist's illustration of a stellar stream is shown in figure 1. How these stars end up positioned like this comes from the dissolution of the progenitor creating the stream. Any cluster within the galactic potential will experience tides caused by the host galaxy. For each cluster within the

galactic potential there will be 2 points where the galactic potential exactly balances the internal gravitation of the cluster called the Lagrange point. Stars travelling near these Lagrangian points can then leave the volume of the cluster and become free from the cluster's own gravitation. The locations of these points will be between the center of the cluster and the host galaxy, and on the opposite side of the cluster, i.e., further away from the galaxy. Stars escaping through these points will then be located at a different radius than the cluster itself, either closer or further away from the galaxy. The escaping stars with low enough kinetic energy will then approximately follow the clusters orbit but at different orbital speeds, dependent on which point they exit through. If they exit on a larger radius, they will orbit slower than the cluster, and faster if it escapes through the point at a shorter radius. These stars will then follow the clusters orbit closely and create a stream-like structure of stars behind and in front of the cluster (Renaud, 2018).

Since the force causing these stars to escape from its cluster is purely gravitational, the trace they leave behind can be used to probe the gravitational field throughout the stream structure both globally and locally. The stream orbit around the galaxy allows us to probe the gravitational field at a global scale. Local inhomogeneities in the stream can be detected such as altered morphology, gaps or variations in the density. These might be due to substructures causing a local disturbance in the gravitational field. Potential substructures that could cause these variations could be large molecular clouds, spiral arms or dark matter substructures (Amorisco et al., 2016).

Figure 2 shows stellar streams detected from Gaia EDR3 for the heliocentric distance range $10 - 30$ kpc in the Milky Way. The colour shows the proper motion of stars. However, stellar streams are hard to detect and these possible variations in streams calls for even closer study. This is also the main reason for using computer simulations. In this thesis we make use of the cosmological zoom simulation VINTERGATAN (Agertz et al., 2021; Renaud et al., 2021a,b) where we will focus on stellar streams. By using a simulation we are not hindered by the limitations of the observational technology, which allows us to look beyond the detection limits as of today. Looking at these processes in a simulation also makes it possible to test if today's theories and models hold up to what is seen in the Universe.

The choice to use a cosmological zoom simulation comes from the physics it is built on. By using a cosmological zoom simulation it is possible to study properties of the stellar streams, satellites and the main galaxy. This is possible since all these objects have been created and developed under similar circumstances and then interacted in this simulation. The simulation is over a volume much larger than the Milky Way. This allows for interactions with multiple smaller galaxies on cosmology-motivated orbits, while also being influenced by the tidal field created by the Milky Way-like galaxy and its surroundings. This creates a more realistic scenario with properties like the Milky Way, than using a simulation of an isolated galaxy. This allows for an analysis that is much more like what is expected in natural processes; yet one must keep in mind that this simulation, like any

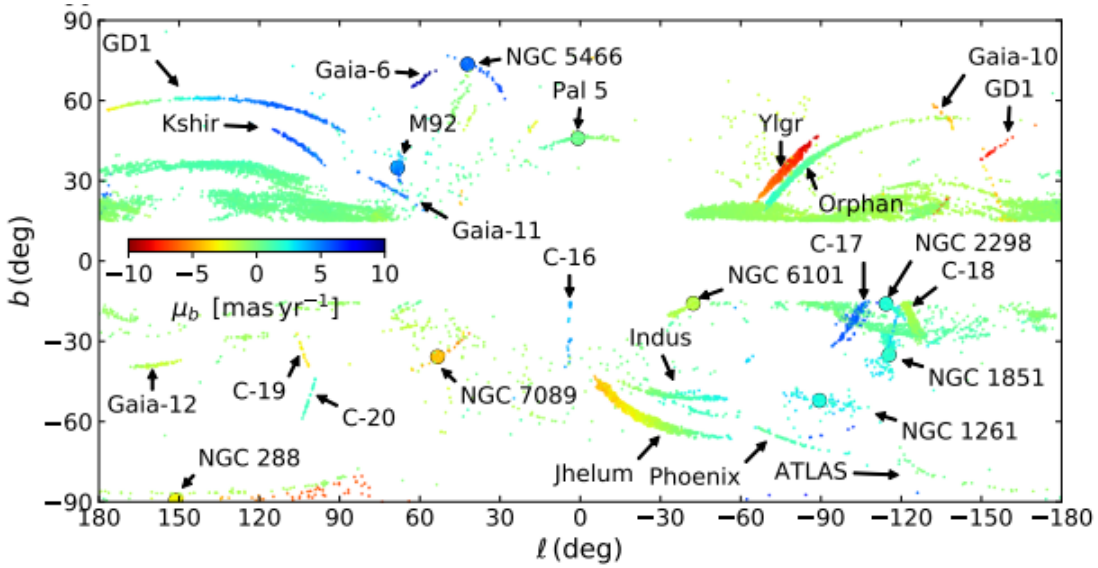

Figure 2: Stellar streams detected around the Milky Way today. The data come from Gaia EDR3 for the heliocentric distance range $10 - 30$ kpc, the colours show proper motions. Figure taken from Ibata et al. (2020).

others, suffers from limitations like limited resolution and incomplete physics. It can give further insight and put real observations into a physical context, while it also allows to identify differences between the simulation and observations.

In this thesis we will investigate the properties of stellar streams and their diversities found in this cosmological zoom simulation. The aim of this project is to understand if streams from these satellites and clusters can be detected within the simulation. The major questions we will address are: do all clusters and satellites produce similar streams? What possible variations and differences exist in these streams and what can cause problems for the detection of the streams? In this thesis we will firstly present the simulation and the analysis methods. Secondly, we will illustrate the methods used to detect the streams. Afterwards, we will describe the properties found in the stellar streams and compare the streams, progenitor, and detection methods. Finally, we will close with a discussion about the methods used and the properties of stellar streams in relation to their progenitors to finally draw the conclusions of the work.

2 Method

2.1 Simulation

The analysis in this thesis is based on the cosmological zoom simulation VINTERGATAN, a detailed presentation of the simulation is described in the three papers (Agertz et al., 2021; Renaud et al., 2021a,b). A summary of the simulation and its data used in this thesis is given below. VINTERGATAN is a cosmological zoom simulation which allows for a high resolution for a main galaxy and its immediate surroundings. The simulation uses hydrodynamics solved over an adaptive mesh refinement grid with the code RAMSES (Teyssier, 2002), in addition to N-body particle-mesh solver for stellar and dark matter particles.

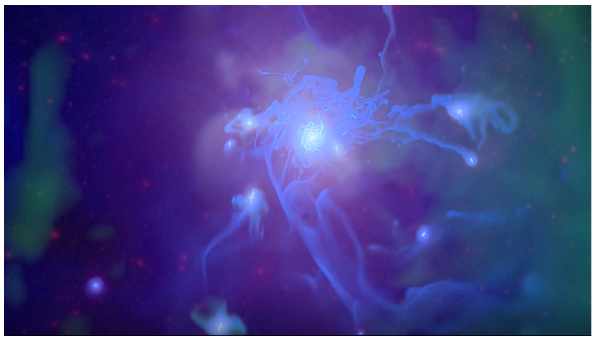

Figure 3: Snapshot taken from the VINTERGATAN simulation and show the last epoch with a redshift $z = 0.17$, which is the analysed time. In this image white represents stars, blue gas, red dark matter particles and green represents iron. Movies of the simulation can be found here[2].

The simulation successfully reproduces a Milky Way-like galaxy with similar mass to the Milky Way. It also produces a similar density profile with 2 populations of stars contained in the thick and thin stellar disc first described in Gilmore & Reid (1983). The simulation also reproduces other key characteristics of the Milky Way such as the rotation curve and the overall chemical composition of stars. Figure 3 displays a snapshot from the simulation during its latest epoch with a redshift of $z = 0.17$, which corresponds to a lookback time of 2.3 Gyr. This is the time of the simulation on which this thesis has done its main analysis on, and from which all the properties of the stellar particles are extracted. Ages referred to in this thesis will be expressed by using the lookback time. In this snapshot the volume of the cube that is extracted has a side length of 350 kpc with the main galaxy at its center. In this volume there is a total of approximately 1.87×10^7 stellar particles with a total stellar mass of approximately $9.0 \times 10^{10} M_\odot$.

The resolution in this simulation is not high enough to resolve individual stars, and instead, we are analysing stellar particles. A stellar particle represents a population of stars which are born at the same time and, therefore, share the same properties such as metallicity, age, and velocity. These particles have stellar masses in the order of 10^3 $M_\odot$. The data extracted from the simulation for this thesis only include the stellar particles with their corresponding properties, therefore, the maps and plots shown in this thesis only

[2]http://staff.astro.lu.se/florent/vintergatan.php

concern the stellar particles and do therefore, not include gas or dark matter particles.

2.2 Data analysis

The data from the simulation have coordinates relative to that of the simulation box itself. The galactic center was computed as the center of mass and velocity of stellar particles within the main galaxy. The spin vector of the galaxy was then computed as the average angular momentum of the stellar particles. The dataset was then centred and rotated such that the galactic center is centred at the origin with the spin vector in the z-direction. The maps are projected from the equivalent position of the Sun. This was done by moving the full system in the x-direction by 8 kpc, hence the galactic center is now located at $(8, 0, 0)$ with the Sun at the origin. A subset of the full dataset is shown in figure 4. Figure 5 shows a projected view of the full dataset with x and y coordinates that correspond to the galactic coordinates (l, b). The map shows the total stellar mass in each direction in $\log(\mathrm{M}_\odot/\mathrm{arcsec}^2)$. The bulge is clearly seen at (0,0), the galactic disc is also visible stretching out on both sides. Multiple satellite galaxies around the galaxy with associated streams can be seen. However, the bulge and disc contaminate the view making it hard to connect some streams with their progenitor. To do more accurate detections of streams from these projected maps the galactic disc and bulge have to be removed.

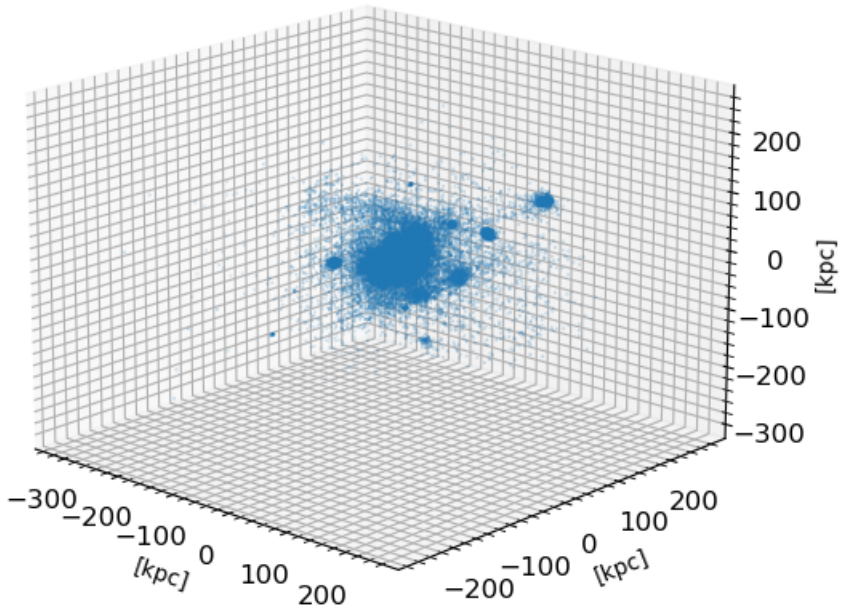

Figure 4: 3D image of a subset of stellar particles from the dataset including 1% of all stellar particles. The main galaxy and some of its satellites are clearly visible.

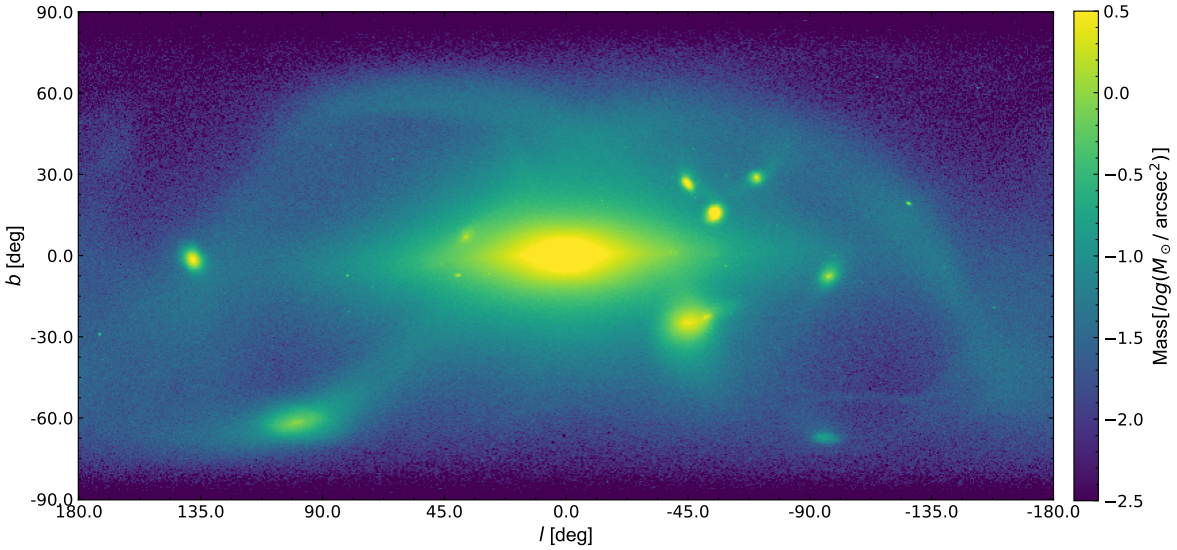

Figure 5: Projected map over the full dataset with galactic coordinates (l, b) on the x- and y-axis. The galactic center is located at $(0, 0)$, here the galactic bulge can be seen with the galactic disc stretching out on both sides. Satellite galaxies and stellar streams can be seen around the main galaxy. The map displays the total stellar mass computed in each direction.

3 Stream detection

3.1 Removal of the galactic disc and bulge

In figure 6 the galactic disc and bulge have been removed. First, all stellar particles in the central region were removed by extracting a cylindrical shape with a radius of 4 kpc and a height of 1.8 kpc. The cylinder was positioned such that its center coincides with the galactic center. This was done to reduce the computational time when later removing the remainder of stellar particles. Then all particles in high density regions were removed by counting the number of neighbours of each star within a given radius. Here stars with more than 1 neighbour within a 0.1 kpc radius were removed. The choice of radius and amount of allowed neighbours was tested using different options. The choice for 0.1 kpc and 1 neighbour was done to get a good extraction of the galactic bulge and disc without extracting tails from the satellites. Due to their high densities, the extraction of the interior of satellites could not be avoided using this method. Figure 6 shows how our method significantly reduces the contamination from the bulge and disc. This is illustrated in figure 7 shows the extracted data. Among the remaining 5.8×10^6 particles, several streams that go through the disc or are located behind the bulge are now easily visible and linked.

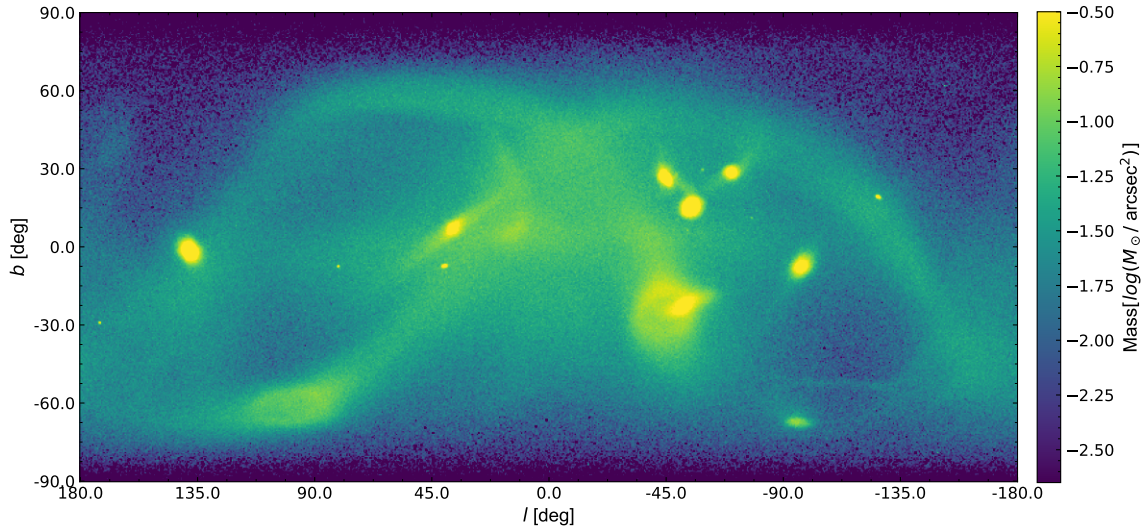

Figure 6: Same projection as in figure 5, but here the disc and bulge have been removed by extracting stars that have more than 1 neighbour within a radius of 0.1 kpc. The bulge and galactic disc have been removed, but this also affects the dense interior of the satellite galaxies.

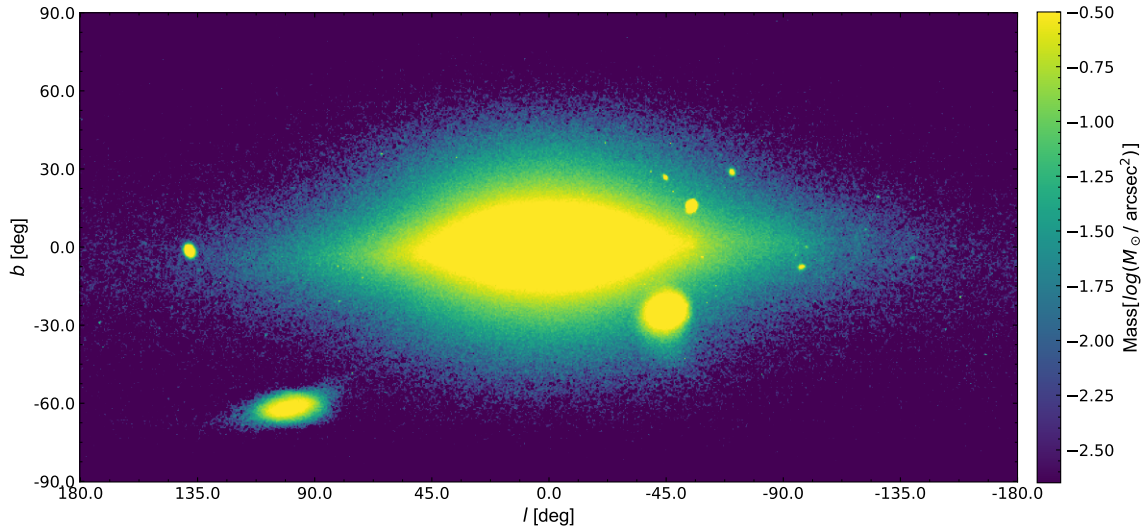

Figure 7: Mass map of the data that have been removed from figure 6.

3.2 Mock observations

We built mock observational data to assess the visual properties of the system and to understand if streams can be detected from surface brightness maps. We assigned a spectrum to each stellar particle using a catalogue of stellar spectra created for single stellar populations. These spectra are depending on the age and metallicity and is created by the code STARBURST99 (Leitherer et al., 1999). This generated a 3-dimensional array with the axes corresponding to wavelength, metallicity, and age. An instrumental filter was then chosen, the filter used here in these plots is g-megacam which can be found here[3]. The choice of filter was based on the wavelength-bands which we expect the streams to be observable in. The combination of g- and r-megacam has been used for the observations of the stellar stream emanating from Palomar 5 in Ibata et al. (2016, 2017). The transmission of our filter was then multiplied by the spectra with the transmission for each associated wavelength. Here the wavelengths that we want to observe in is selected with the associated transmission. The transmitted normalised absolute flux in the chosen band was obtained by integrating over the spectra as seen in equation (1),

$$F_{trans} = \int_{\lambda_{min}}^{\lambda_{max}} T_{filter} \times F \ \mathrm{d}\lambda. \tag{1}$$

Here T_{filter} is the transmission of the filter, F is the flux of a single stellar population, and λ is the wavelength where we integrate from the minimum to the maximum wavelength of the filter. This was done for all metallicities and ages. Then each particle was assigned a spectrum depending on the metallicity and age. Finally, the denormalised absolute flux was obtained by multiplying with the stellar mass. Apparent flux was obtained by taking the distance to each stellar particle into account. The surface brightness maps of our system are then computed by binning the fluxes and normalise by the angular size of the bin. These are seen in figure 8 and 9 without and with the removal of disc and bulge respectively.

Figures 8 and 9 show the apparent magnitude per arcsec^2 of the simulated system. In figure 9 we removed the contribution from the disc and bulge. However, even in these favourable conditions any structures or streams are very hard to detect, and the remains of the disc still outshine any structure in the halo. In figure 9 we still observe the presence of the part of the galactic disc and the two nearby satellites. One stream can be seen from the satellite located at $(90, -60)$, but it is hard to identify any other structure. The main factor causing this is the distance to the streams and satellites, since they are located much further away relative to the stars in the galactic disc. This is illustrated in figure 10 where the absolute magnitude of the system per arcsec^2 is shown. It is apparent that if we only consider the absolute magnitude of the system (i.e. ignoring the distances) we can produce a similar plot as in figure 5, where most structures are visible. To detect streams in these surface-brightness maps, more advanced detection methods have to be used. This is beyond the scope of this project, and instead we adopt some alternative methods.

[3]https://astrom-tom.github.io/SEDobs/build/html/filters.html

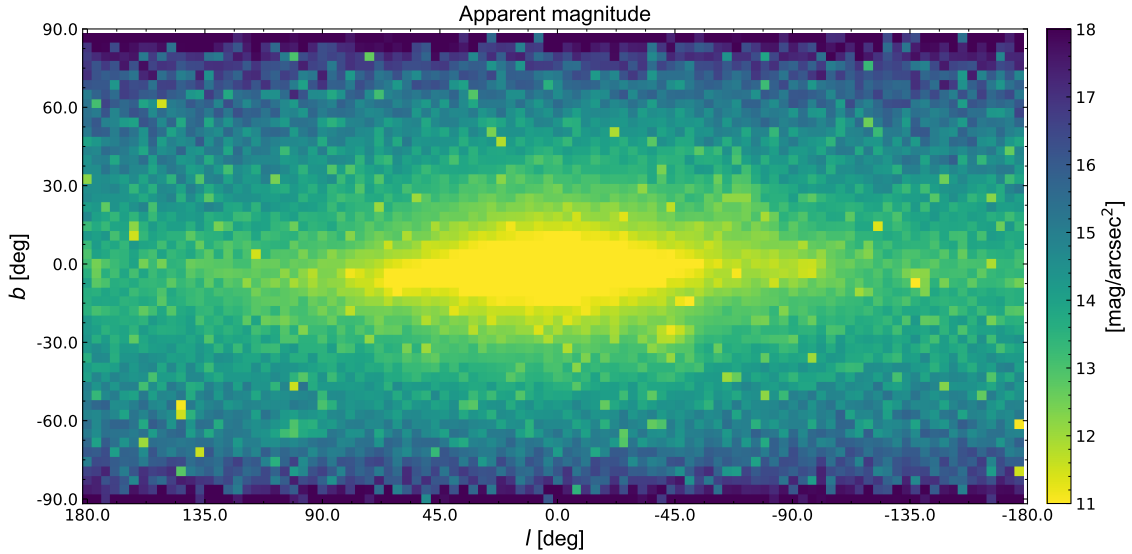

Figure 8: Surface brightness map over the full system. It is clear that the bulge and disc outshines the galaxies and that it is difficult to detect any structure far away from the disc.

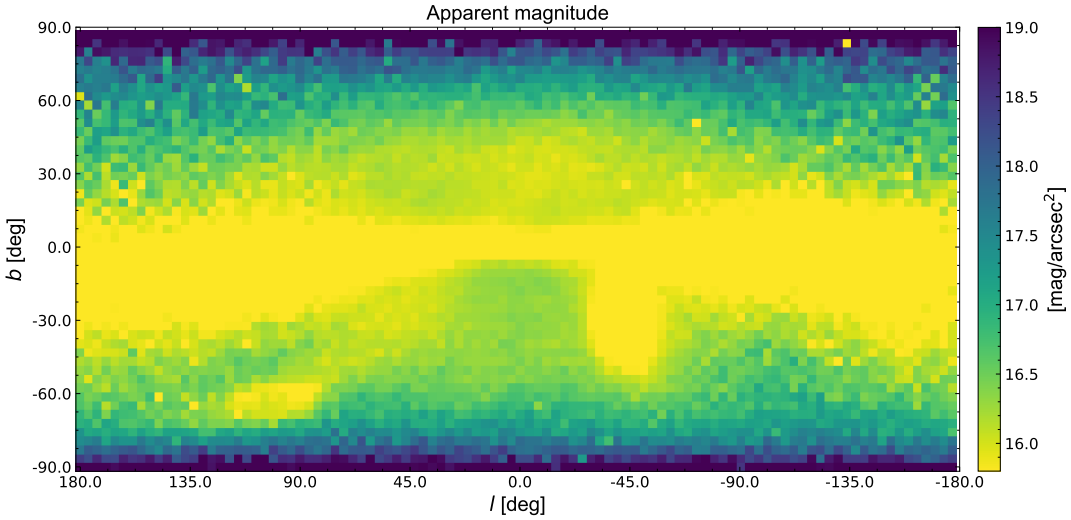

Figure 9: Same projection and filter as in figure 8. Here we adopt a different colour scaling and the galactic disc and bulge are removed. The remains of the disc still outshines the galaxy. Nearby clusters are seen, including one with a corresponding stream. Its progenitor is located at $(90, -60)$.

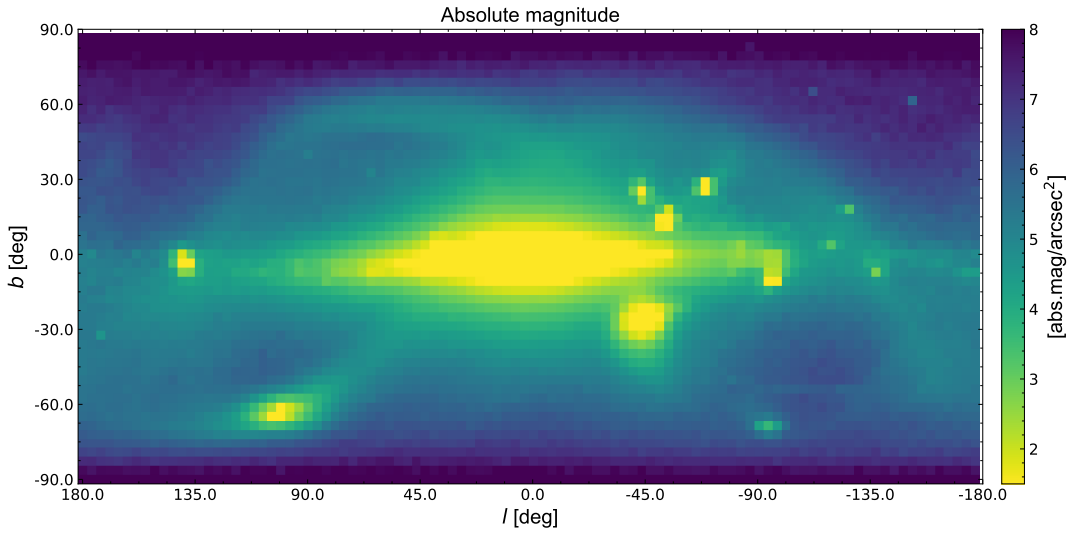

Figure 10: Projected map with absolute magnitude per arcsec^2 for all stars. Here it is clear that the absolute flux from streams can be seen in the full data set, but taking the distance into account makes the nearby stars outshine all distant structures. Hence, the main contribution of the difficulties to detect streams originates from the distance and not from age or metallicity of stars.

3.3 Alternative methods

We used different alternative methods to detect streams. Depending on their properties, location, and velocities the streams can be more visible in some spaces compared to others, with spaces referring to for example metallicity, distances, radial velocities, energy. In figure 11 the normalised average distance is combined with the normalised stellar mass. This was done by creating two arrays one with mass and the other with average distance. Each bin covering a specific angular size on the map and computing the total stellar mass in each bin. All bins exceeding a specific mass was assigned this specific value and later normalised. For the other array, the average distance in each bin was computed and normalised. These two arrays were finally added to each other to create the combined image. The normalisation was done to make both quantities have a similar contribution to the map. Using this map both distant and nearby structures can be emphasised. Many of the satellites and clusters in this image show stream structures, but not all. One reason for this could be that their streams are very diffuse and therefore not visible in these maps. Another reason could also be the resolution of the simulation, since it does not resolve individual stars and streams with a small mass might not be produced in this simulation. Finally, it is also possible that the streams have not formed yet, for instance if the satellite is still on an incoming trajectory.

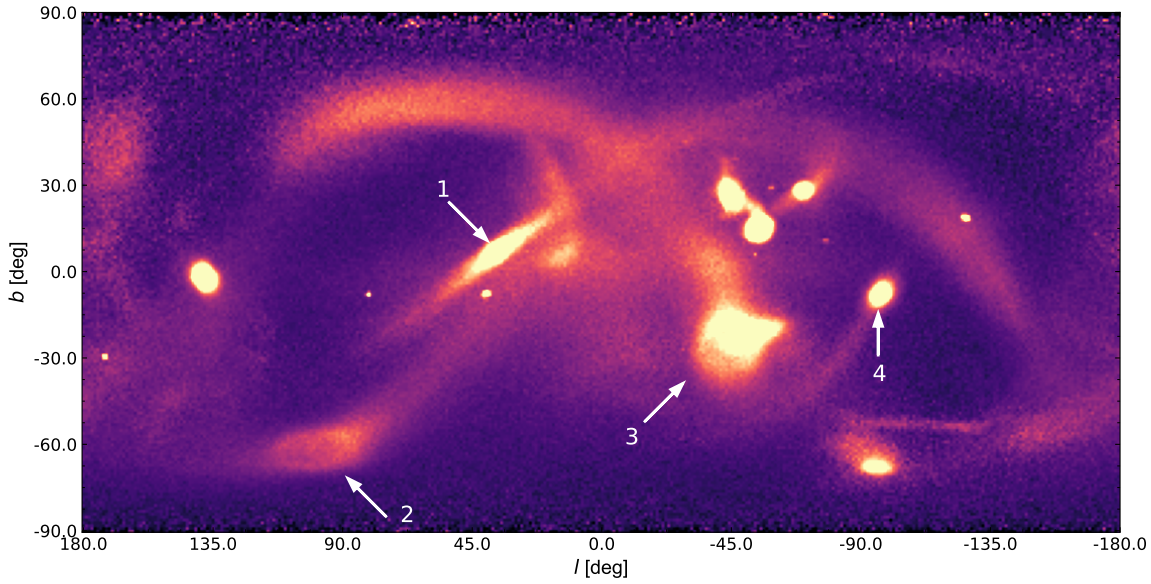

Figure 11: A combined image over normalised stellar mass and distance. Here both distant and nearby structures can be seen. Multiple structures and streams are seen in this image. The progenitors to the streams detected and analysed in this thesis are shown by their corresponding number. Interestingly, not all clusters and satellites seems to have a corresponding stream.

We use multiple methods to detect streams, reasons for this are that some methods are closely related to what is done in observations. Other methods used here are not possible to reproduce in observation but can be used in simulations for better analysis and comparisons between the different methods. The other method used here is very accurate, however it is not possible to be reproduced in observations. It is, nevertheless, useful to compare the properties of the detected streams. Our first selection of streams will be from detection methods that are closely related to real observational methods.

The structure we label as stream 4 was detected by looking at the metallicity of stars relative to the radius. The stars selected have a close to primordial metallicity where the selected range in [Fe/H] is $[-52, -50]$. The exact value of [Fe/H] is subject to details of the implementation of the initial physics in the simulation and will not be further discussed here. The range in radius selected for these stars had a lower limit of 50 kpc and without an upper limit. The stars were seen as a group at 75 kpc from the galactic center with a smaller density of stars sparsely separated at larger radius.

Three streams were detected in the phase-space distribution of stars shown in figure 12. Stars are presented in the total energy E_{tot}, and angular momentum L_z, being perpendicular to the disc. However, the very large volume of data extracted from the simulation

does not include the potential, which must then be retrieved from the grid. However, determining in which cell each of the particle lie is prohibitive from the point of view of the computational cost. Re-computing the potential would have required accounting for the many resolution elements in the gas and dark matter, also at a prohibitive cost. For this reason, the resolution of the grid has been degraded, and we considered only 1 out of 50 particles. This leads to an approximate and partial result, insufficient to reflect the full structure of the galaxy, but still allows us to detect some streams.

In figure 12 the phase-space distribution is presented. The saturated area around $L_z = 0$ corresponds to the overall galaxy that is left. One structure in particular stand out, located in the bottom left and corresponding to stars seen in stream 1 in figure 13. The structures seen as streams 2 and 3 in figure 13 are showed by the arrows 2 and 3 respectively. Stream 1 that was a clear outlier and located separately from the rest of the galaxy got a clean extraction and contains a low amount of contamination. However, for streams 2 and 3, both originating from much larger satellites and closer to the galaxy, parts of their progenitor have been lost during the removal of data. These progenitors can be seen in figure 11. They also contain some more contamination from nearby stellar particles being with similar phase-space distribution.

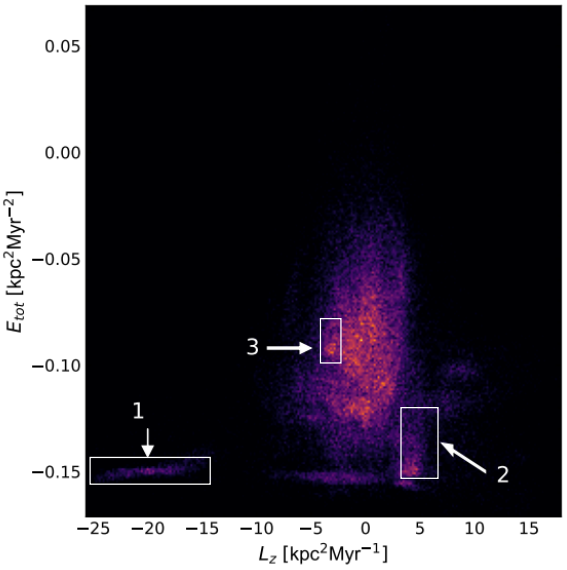

Figure 12: Phase-space distribution of a subset of stars with the total energy, E_{tot}, plotted against the angular momentum in the z-direction, L_z.

The previously used detections methods are similar to methods used to analyse observations. These streams and their properties are later compared to streams from a second selection. This second selection is based on the streams that have already been detected, but here the satellite and stream is tracked starting from 1.6 Gyr before than the currently used data. This is before the infall to the galaxy of the satellites associated with streams 2 and 3, hence these stellar particles are tracked back to their original progenitor. The main reason for this was to create better stream detections to compare with the first selection. For streams 2 and 3 their satellites were still intact and no prominent stream structures could be seen at this epoch, hence all stars within their satellites could be selected. However, for stream 1 and 4 which already had prominent streams at this time nearby stars were included in this selection. This was done since they were located far from the main galaxy and therefore, should not include too much contamination. Stream 1 and 4 there-

fore, contain a smaller amount of contamination when traced back to this epoch, but now contain many more stellar particles allowing for better analysis while also having intact progenitors. The resulting streams from this selection made in an earlier snapshot is seen in figure 14. A noticeable difference with respect to the results of the previous is that streams 2 and 3 have a clearly visible satellite and stream, which were instead almost removed in the first selection. By using this second selection the number of stellar particles increases drastically and enables a much more complete analysis of the properties of the streams.

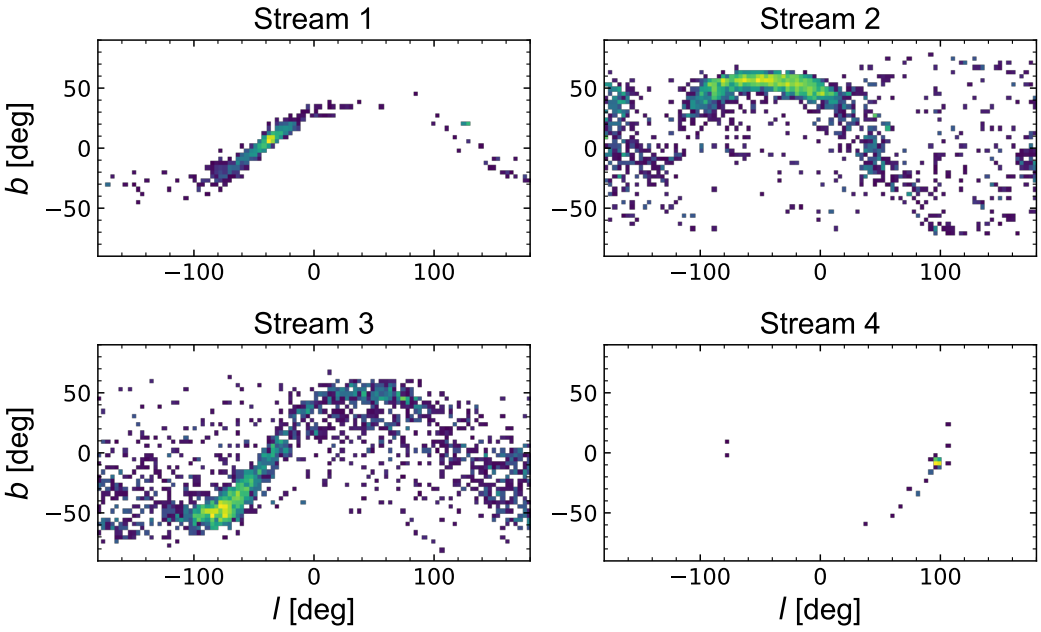

Figure 13: Streams 1-3 detected in the phase-space distribution in figure 12 shown in (l, b) coordinates. All streams contain some contamination from nearby stars in the phase-space distribution. Streams 2 and 3 include more contamination of nearby stars. Stream 4 was selected as a group of stars with a very low metallicity.

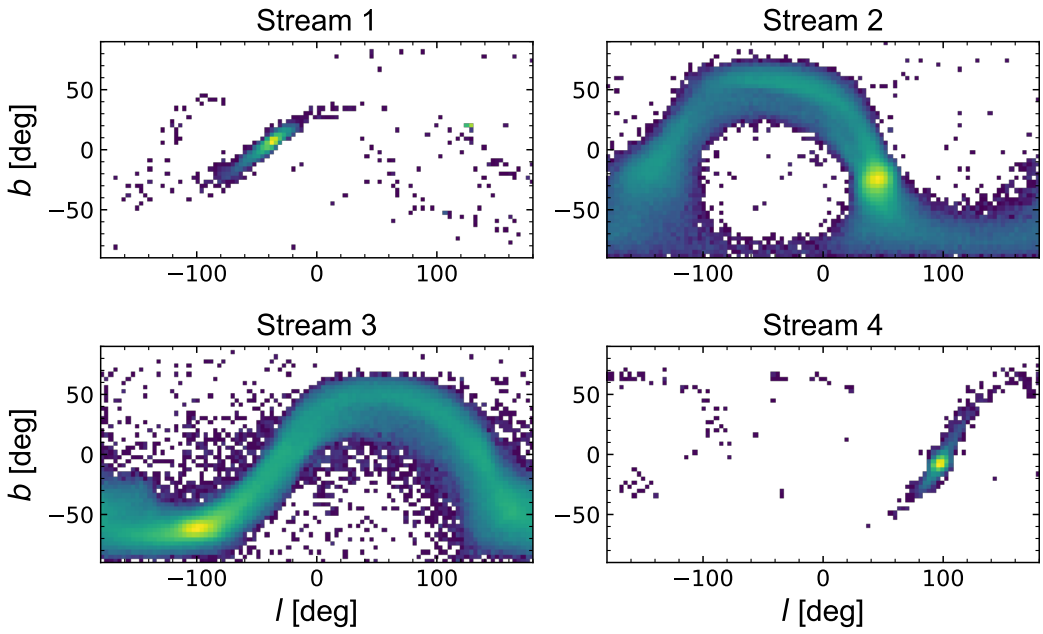

Figure 14: Stars traced back from their satellite or stream from an epoch 1.6 Gyr before the latest snapshot. Here the progenitor of the streams can clearly be seen and the amount of stars is increased.

4 Stream properties

4.1 Stream masses

The stellar masses of the streams are presented in table 1. The masses of streams 2 and 3 were obtained by computing the stellar masses of all particles within a spherical volume centred on the satellite before the infall into the galaxy. For streams 1 and 4 which had already prominent streams at the early epoch, nearby stellar particles were selected to capture the majority of the satellites and missing stars within the stream. Hence, these streams masses do not correspond to their current stellar masses, and instead refers to the masses of the progenitor and stream from the early stage in their evolution.

Table 1: The masses of the streams computed as the masses of the satellite before the infall to the galaxy.

Stream 1 [$M_\odot$]	Stream 2 [$M_\odot$]	Stream 3 [$M_\odot$]	Stream 4 [$M_\odot$]
2×10^8	3×10^9	2×10^9	2×10^8

4.2 Star formation history

The age distribution is presented in figure 15 for the first detection method applied. Stream 4 is not included in this plot since the selection only included a small range in metallicity, corresponding to an age of approximately 12.5 Gyr. One feature that stands out is that all streams show a bimodal age distribution. In stream 1 there are 2 peaks in the age distribution indicating that star formation stopped 11 Gyr ago and started again at 9 Gyr. Stream 1 does not have any stars with an age smaller than 5 Gyr. Stream 2 also shows 2 peaks, but with a different shape and no stop in star formation. Instead, it shows that star formation slowed down 10 Gyr with a second peak at 8 Gyr, but then goes through an abrupt stop in star formation $7 - 8$ Gyr ago. Stream 3 shows a much smaller peak at around $8 - 9$ Gyr and a peak at 11 Gyr, where both of these peaks gradually decrease compared to stream 2.

The second selection shows some different characteristics of the age distribution in the streams (see figure 16). Here the stellar mass within the progenitor is also shown for a few reasons. First, we see star formation histories which differ from those found with the other technique, especially in stream 2. Here we see that the second wider peak around $10 - 12$ Gyr is not included in the second selection. Second, to evaluate if the properties of the progenitor are different to that of the stream. Lastly, the first selection used is done on the degraded resolution, the removal of particles had a greater effect on the progenitor relative to the stream and therefore some features can be missed.

Looking at stream 1 an increase in number of stars within the first peak is seen. This most likely originates from the fact that the progenitor itself has been stripped of stars at its center where we expect most of the younger stars to be located, but the stream itself is not as affected by this. Also, some younger stars can now be seen in the stream younger than 5 Gyr. These most likely come from some contamination in the volume selection in the early epoch. Looking at stream 2, there is now only one sharp peak seen at 8 Gyr,

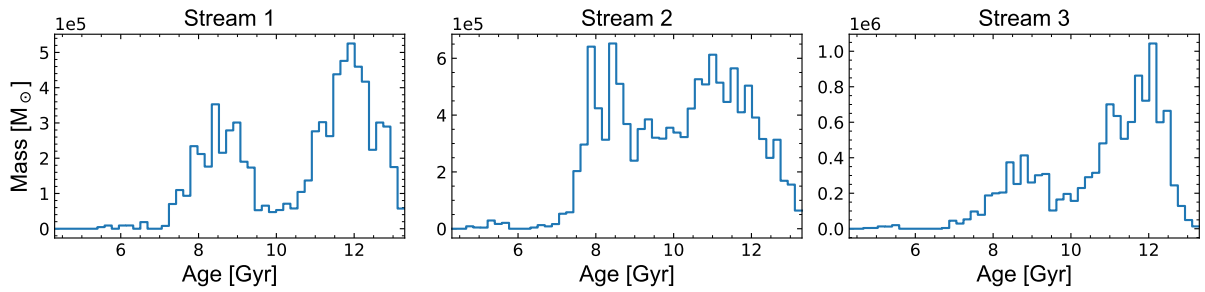

Figure 15: Stellar age distribution in streams from the first detection method. All streams show a bimodal age distribution where all show a peak at around $8 - 9$ Gyr. However, they all show very different star formation histories.

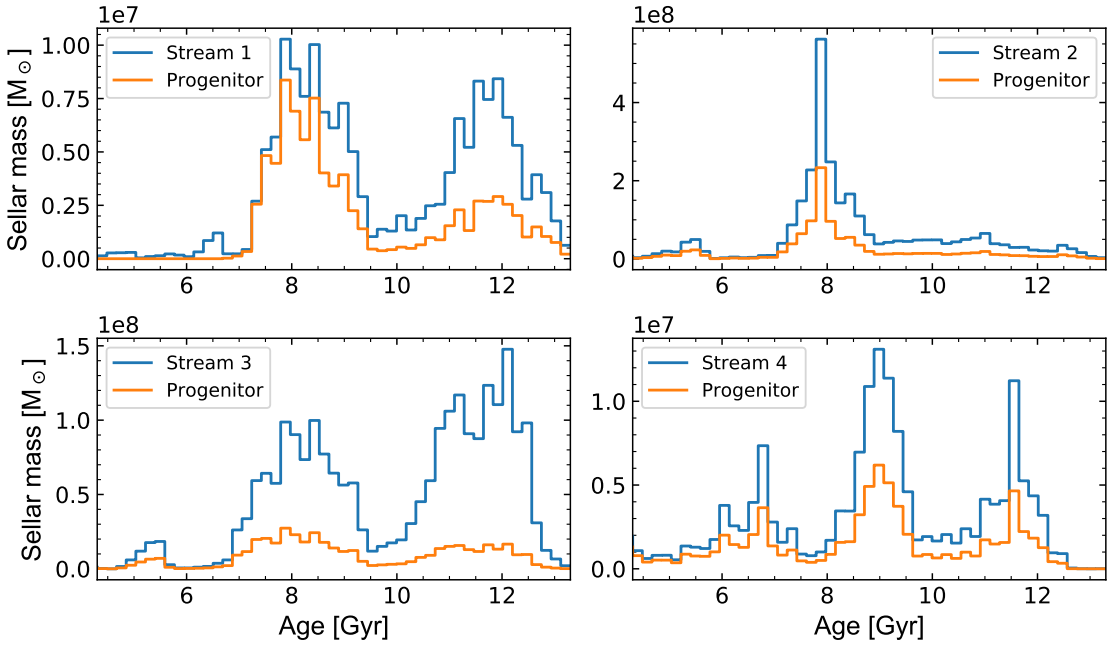

Figure 16: Stellar age distribution found in each stream and in their respective progenitor by applying the second selection method is displayed. Multiple differences can be seen from the age distribution shown in figure 15, the most noticeable change is seen in figure 2 where the peak at 12 Gyr is gone.

which can indicate that there is a lot of contamination in the first selection giving it an extra peak. Stream 3 shows the same characteristics as in the first selection with the exception that the peak around 8 Gyr contains a larger fraction of stars since the progenitor is more intact. This is probably caused by the extraction of stars in the progenitor in the first selection. Stream 4 which was detected from old stars with a primordial metallicity now shows 3 peaks. As can be seen in figure 14 it also shows some level of contamination as seen for stream 1. These two streams already had prominent streams in the previous snapshot with respect to $t = 1.6$ Gyr, hence selecting the volume of the cluster would miss the stars within the stream, therefore neighbouring stars was included which have caused some extra contamination.

The stellar age plotted against the distance from the progenitor is shown in figure 17. Streams seem to be dominated by older stars, but still, we find a high diversity of ages within the progenitor. Stream 2 shows a great diversity in both the stream and progenitor. Comparing this with the age distribution in figure 16, we see that most stars were born around 8 Gyr ago and this diversity within the stream can be partly caused by contamination. However, they all show a clear trend with younger stars near the progenitor. The stripe seen in both figure 17 and 18 at large distance in stream 1 is likely contamination from a cluster at a similar position in the phase-space distribution.

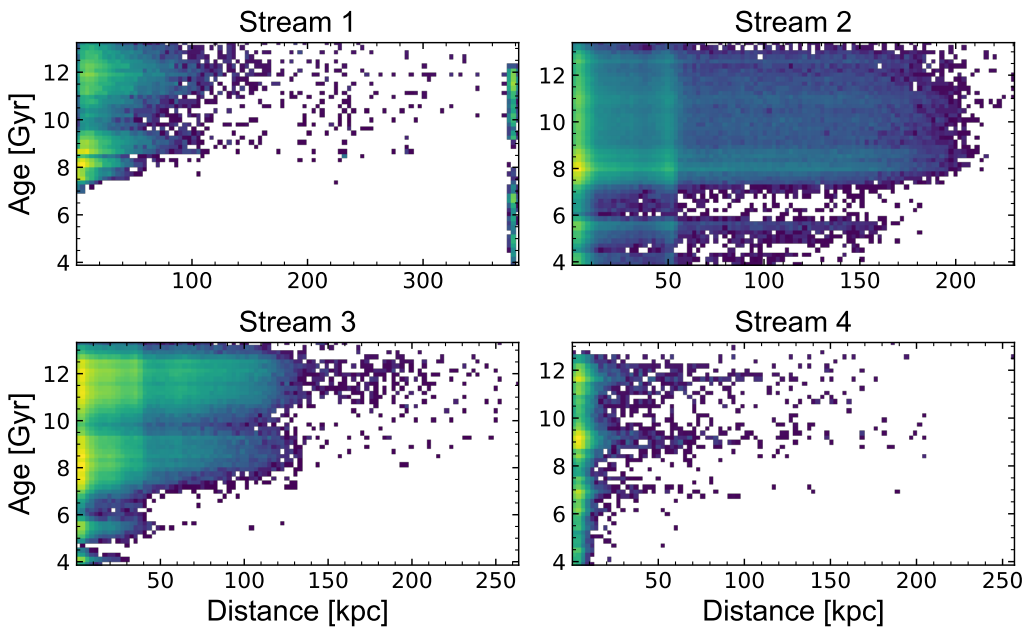

Figure 17: Stellar age plotted against distance from the progenitor using the second detection method. It shows that older stars seem to dominate in the streams compared to younger stars still in the progenitor. The stream still shows a great diversity in the stellar age.

4.3 Metallicity in streams

In figure 18 the stellar metallicity is plotted against the distance from the progenitor. All streams show a diversity in their metallicities. The progenitors contain a wide range of metallicities compared to the streams: the range in metallicity decreases as the distance increases. An interesting feature is that the streams do not contain a high fraction of stars with low metallicity. This would be expected from the fact that older stars should dominate within the stream and on average contain a lower metallicity. The most massive streams, that are streams 2 and 3, show a greater diversity and a higher metallicity compared to streams 1 and 4. This can be compared with their age distribution. In the age distribution for stream 1 there is barley any ongoing star formation after 5 Gyr. Stream 4 however, shows multiple peaks that may come from contamination. One explanation for the lower metallicity that stream 1 and 4 have in common is the mass of their satellites as stream 1 and 4 are of lower mass. Hence, there could be a way to trace the masses of the original satellites by looking at the metallicites of their streams, but this is not yet quantified.

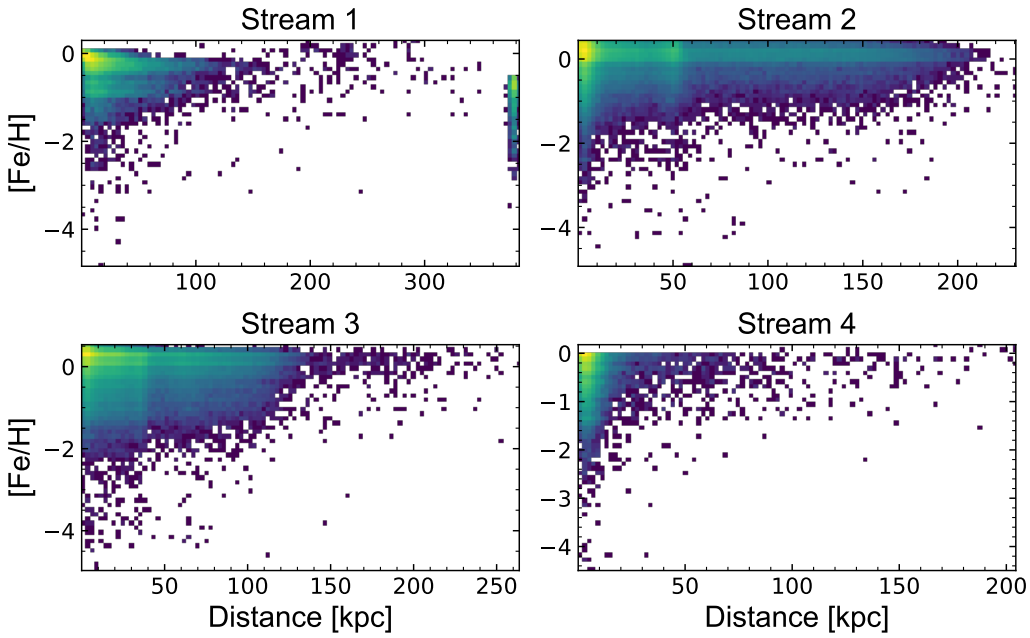

Figure 18: Metallicity plotted against the distance from the progenitor for each stream. Stream 1 has some degree of contamination originating from a cluster at large distance which is seen as a stripe at almost 400 kpc. The diversity in metallicity is greater in the progenitor than in the stream. Stream 1 and 4 have a large diversity, but a lower metallicity as stream 2 and 3.

5 Discussion

5.1 Limitations

The simulation does not resolve individual stars and therefore, we limit ourselves to the analysis of stellar populations. Therefore, our results can not be directly transposed onto stellar streams detected in the Milky Way. The stellar masses of the progenitors of the streams analysed here are of the order $10^8 - 10^9$ $M_\odot$ measured as the stellar mass of the progenitor before the infall to the galaxy. These masses are similar to the most massive streams and their progenitors detected in the Milky Way today, such as the Magellanic Stream. However, this stream is mainly made of gas (D'Onghia & Fox, 2016), and in this thesis we only look at the stellar components of these satellites and not at the gas or dark matter that the satellite or stream might contain. Looking at smaller streams in this simulation we can compare this with streams originating from globular clusters in the Milky Way. These have an average mass in the order of a few 10^4 $M_\odot$ (Baumgardt & Hilker, 2018), comparing this with the resolution of stellar particles with masses 10^3 $M_\odot$. One reason for the lack of small streams detected could then be the limited resolution causing smaller clusters and satellites to not produce any streams. The smaller satel-

lites that are visible in the (l, b) space have a stellar mass in the order of $10^6 - 10^7 M_\odot$ which is much larger than the mass of an average globular cluster in the Milky Way. More time would have been necessary to find streams from these low mass satellites and clusters.

The method used for the energy and momentum selection required a low resolution leading to a loss of stellar particles where some important features of streams and progenitors might have been lost. This problem arose from the computational cost it took to scan the potential in the grid for each particle in the simulation and a degradation of the grid was done and only a smaller fraction of the particles was taken into consideration. This could have been avoided by using an analytical approach for the potential by using a more simplistic model. However, there could be new problems with this due to the potential of the galaxy having a fine structure that would be missed as well as any non-axisymmetries within the potential would be missed as well. This could lead to other problems with the detections of streams where false positives might arise. This method was, however not tested and only the low resolution dataset was used. Further analysis could be made to see if these detection methods could have been improved with a different choice for the treatment of the potential.

Nevertheless, 4 streams were analysed, with more streams being visible in the simulation. The goal for this project analysis was never to find any statistical results, but rather to illustrate some aspects of these streams, like the star formation histories, differences between progenitor and stream and differences between the detected streams. A great variety in stream properties were found in their metallicity, mass, star formation history and visibility. We have shown a great variety in one of the massive streams detected, stream 3, but also for stream 1 and 4 which have a significantly smaller mass. We also see differences in their respective metallicity in the progenitors and stream in figure 18 where the smaller streams 1 and 4 do not show as high metallicity compared to streams 2 and 3.

5.2 Detection methods and properties of streams

In this simulation stellar streams have been detected around many, but not all satellites and clusters. For some satellites and clusters the streams are either very diffuse or non-existent. Therefore, some parts of their history could be hidden if their stream is too faint to be detected. There could be multiple reasons for the fact that these streams are not visible. The simulation used in this thesis has a limited resolution and does not resolve individual stars. These stellar populations have masses is the order of 10^3 $M_\odot$ and can therefore, affect the formation of streams from these smaller satellites.

Looking at the streams detected in this thesis we see long tails from both stream 1 and 4 when isolated in figure 13 and 14, but these long tails are very hard to see visually in any of the other (l, b) plots presented. The full length of stream 1 could be obtained due to the clear separation in the angular momentum in the z-direction from the rest of the galaxy. This could, however, not be done for stream 4. This stream is faint and contains a small

number of stars relative to the more massive streams 2 and 3. Comparing the two stream selections of stream 4 in the figures 15 and 16, we find that most of the stream is missing in the first selection. This is mainly a consequence of selecting stars within a narrow range in metallicity or age when looking for the streams. As seen in the star formation history of this stream detected in the second selection (see figure 16) we see that no complete stream detection can be made from selecting in one range of metallicity or age. Hence, in the case of lower mass streams which contain a diversity of stars, different detection methods are needed to get a more complete detection of the stream.

The detection of stream 2 in the first selection contains a large amount of contamination. Only a partial detection of the stream could be done. This stream and its progenitor are heavily affected by the degraded resolution of the data, and this might have caused problems for the detection done using the phase-space distribution. Having a more intact progenitor might make the over densities easier to detect. The extraction made using the phase-space distribution included some contamination from another satellite which was removed considering the radial velocity of the satellite. However, using all these parameters a partial stream could be extracted, but the result is far from being perfect. This was clearly illustrated when comparing the two selections and their respective star formation histories. Here some clear inconsistencies could be seen. Another interesting property of this stream is that the star formation history shows a lot of similarities between the progenitor and the stream, which is not seen for stream 1 and 3.

In contrast to stream 2, the other more massive stream, stream 3 shows a very different history. One clear difference looking at figure 16 is that the stellar populations within the stream are different to that of the progenitor. This stream is also dominated by the older stellar population, however, here the progenitor has a higher fraction of the younger stellar population. This makes sense since stars are born near the center of the satellite and, therefore, the outskirts of the satellite will contain a larger fraction of older stars. This is also shown by the results concerning the star formation history of stream 1 and 3. Therefore, transposing the properties of the progenitor onto the stream can lead to errors if one were to use this approach for the stream detection. This is due to the fact that the stream might show other properties that would be missed by studying the progenitor alone.

Lower mass clusters and satellites in this simulation which are not showing any visible streams might be explained by their streams being too faint to be detected or by the fact that low mass systems do not produce any stream. If we look closely at stream 1 and 4 there are long tails which are not seen visually in any of the (l, b) plots presented except for the ones where they are isolated. Therefore, these small satellites and clusters who are not showing any streams could have long tails that are too faint to be detected with the methods used. Smaller satellites might have detectable streams in the phase-space distribution when a higher resolution is considered. What could be done to see if they are detectable is to look at these satellites before the infall to the galaxy. In a similar way as done to create figure 14, it would be possible to see if they do create a stream or not, how

faint they are, how long tails and possibly how they could have been detected. This process would, however, only be possible in artificial experiments and can not be reproduced in the Milky Way. However, it could still give information about which streams that are created and which are not within this simulation while also providing constraints on the stream production. With these reasons in mind smaller satellites might not create any streams at all due to the resolution of this simulation. Stellar particles in the mass ranges thus simulation might not leave these smaller clusters such as streams are created by globular clusters in the Milky Way.

6 Conclusion

In this thesis a cosmological zoom simulation of a Milky Way like galaxy has been used to detect stellar streams. Multiple detection methods have been used to detect stellar streams. First surface brightness maps were used to evaluate how this system looks. This showed that the bulge and galactic disc outshines the galactic halo, and no stream detections could be made from this method. More advanced methods would be needed to distinguish structures at larger distances. The same results were seen even in more favourable mock observations where a large part of the galactic disc together with the bulge had been removed.

In figure 11 a map is presented showing the stellar mass combined with the average distance. This illustrates that most streams are visible in this system without any deeper analysis. The most massive satellites and clusters do have corresponding streams, but a large fraction of the smaller clusters does not have any visible streams at all. This could be a numerical effect or a consequence of the fact that these streams are too diffuse to be detected through the methods used in this thesis.

However, four streams were detected with various properties. There are multiple differences between the streams analysed in this thesis. The visibility of streams is very different, both within the stream structure and between the different streams. The age distribution is different for all streams that show different histories. The first stream detected shows two peaks in its star formation history where most of the old stars are now contained in the stream, while the younger stellar population dominates within the progenitor. A similar distribution was found for stream 3 as well. However, for stream 2 and 4 the interpretation of the results is not as clear. Here both the progenitor and stream seem to have a similar distribution.

As a result of this work, it has been shown that a diversity in stellar streams can trace the history of star formation and accretion of its progenitor. However, the stream and the remains of the progenitor can show different stellar populations, therefore, information

about both structures are needed for a conclusive result. It has also been shown that a partial detection of stellar streams should be interpreted carefully and not lead to rapid interpretations of the diversity of the full stream and progenitor.

As a next step we will use a higher resolution to calculate the energy and the potential to improve the stream detection methods. Being able to retrieve the entire satellite might have led to different results. A deeper analysis focusing on smaller satellites might show fainter streams in this simulation. As seen in stream 1, these faint streams can still stretch over very large distances. A possibility to see if they are detectable and how to detect them could be to trace these satellites and clusters from an earlier epoch as done, similarly to what we have done in figure 16 for the detected streams.

References

Agertz O., et al., 2021, MNRAS, 503, 5826

Amorisco N. C., Gómez F. A., Vegetti S., White S. D. M., 2016, MNRAS, 463, L17

Baumgardt H., Hilker M., 2018, MNRAS, 478, 1520

D'Onghia E., Fox A. J., 2016, Annual Review of Astronomy and Astrophysics, 54, 363–400

Gilmore G., Reid N., 1983, MNRAS, 202, 1025

Ibata R. A., Lewis G. F., Martin N. F., 2016, ApJ, 819, 1

Ibata R. A., Lewis G. F., Thomas G., Martin N. F., Chapman S., 2017, ApJ, 842, 120

Ibata R., et al., 2020, arXiv e-prints, p. arXiv:2012.05245

Leitherer C., et al., 1999, The Astrophysical Journal Supplement Series, 123, 3–40

Renaud F., 2018, Nar, 81, 1

Renaud F., Agertz O., Read J. I., Ryde N., Andersson E. P., Bensby T., Rey M. P., Feuillet D. K., 2021a, MNRAS, 503, 5846

Renaud F., Agertz O., Andersson E. P., Read J. I., Ryde N., Bensby T., Rey M. P., Feuillet D. K., 2021b, MNRAS, 503, 5868

Schumann M., 2019, Journal of Physics G Nuclear Physics, 46, 103003

Springel V., et al., 2008, MNRAS, 391, 1685

Teyssier R., 2002, A&A, 385, 337